Relevance of Absolute and Relative Energy Content in Seismic Evaluation of Structures

Erol Kalkan[1] and Sashi K. Kunnath[2,*]

[1]California Geological Survey, Earthquake Engineering Program, Sacramento, CA 95814
[2]Department of Civil and Environmental Engineering, University of California Davis, Davis, CA 95616

(Received: 20 November 2006; Received revised form: 23 April 2007; Accepted: 14 August 2007)

Abstract: A reassessment of input energy measures taking into consideration the characteristics of near fault ground motions is presented. The difference between absolute and relative energy input to structural systems is shown to be more significant for near-fault than far-fault records. In particular, the coherent velocity pulse contained in near-fault records resulting from a distinctive acceleration pulse rather than a succession of high frequency acceleration spikes produces sudden energy demand in the early phase of the response and is typically larger than the total energy accumulated at the end. Studies using idealized pulses indicate that input energy is a function of the shape and period of the velocity pulse. For spectral periods shorter than pulse period, greater absolute energy is input into the system rather than relative energy, while the reverse is true for spectral periods larger than the pulse period. The discrepancy between two energy definitions is initiated by the phase difference in ground velocity and system relative velocity, and it tends to be minimal as the pulse period approaches to system vibration period. The significance of these findings, based on linear SDOF simulations, is further investigated by examining the nonlinear seismic response of a group of realistic buildings subjected to near-fault recordings with and without apparent acceleration pulses. This study concludes that selection of appropriate energy measure for near-fault accelerograms should be based on the shape and period of dominant pulse in the record, and the vibration properties of the structural system.

Key words: seismic input energy, velocity pulse, acceleration pulse, near-fault, directivity.

1. INTRODUCTION

Since the mid 1950s when Housner (1956) addressed concepts in limit-state design methodology and recognized the need to provide adequate energy-dissipation capacity to structural components, energy-based design approaches have gained considerable attention. Several papers that utilize energy-based concepts in evaluation and design have been proposed in the past (Park et al. 1984; Krawinkler 1987; Tembulkar and Nau 1987; Minami and Osawa 1988; McCabe and Hall 1989). However, the definitive work that re-examined the concepts of relative and absolute input energy and renewed interest in using input energy as a potential measure of structural demand was the paper by Uang and Bertero (1990). Their work demonstrated the importance of absolute input energy and identified the presence of large spikes in the energy time-history. Since then, a great deal of effort has gone into the estimation of energy demands and dissipation mechanisms in structures resulting in the development of energy based spectra (Decanini and Mollaioli 2001; Chou and Uang 2000; Chai and Fajfar 2000; Riddell

*Corresponding author. Email address: skkunnath@ucdavis.edu; Tel: +1-530-754-6428

and Garcia 2001; Kalkan and Kunnath 2006) and input-energy-controlled procedures for seismic design (Otani and Ye 1999; Leelataviwat et al. 2002; Chou and Uang 2003). The fundamental premise behind energy-based design methods are that energy dissipation capacity of structural elements can be established based on the predicted energy demand from earthquakes. To quantify the energy imparted to structures, both relative input energy and absolute energy definitions have been used. Fajfar and Vidic (1994), Riddell and Garcia (2001) and Ordaz et al. (2002) used relative input energy in their work while Berg and Thomaides (1960), Goel and Berg (1968), Mahin and Lin (1983), Teran-Gilmore (1998), Chapman (1999) and Takewaki (2004) opted for measures based on absolute input energy. However, none of these studies explicitly consider ground motion characteristics in distinguishing the relative or absolute input energy definitions.

This paper re-visits the two input energy definitions in light of the recent findings related to near-fault ground motions. Given the large number of near-fault records that are now readily available, this study aims to add to the knowledge of directivity effects on imparted energy to structures. Near-fault records having either fling effects or forward directivity are judiciously selected from different seismic events with particular emphasis on acceleration pulses. Recent studies of near-fault ground motions (Hall et al. 1995; Heaton et al. 1995; Iwan 1997) have generally paid more attention to velocity pulses alone thereby overlooking the acceleration content that leads to the build up of the velocity pulse. In fact, the significance of localized acceleration pulses in generating damage was pointed earlier by Takahashi (1956) and later by Bertero (1976). Recently, acceleration pulses have been mentioned in the studies of Bonelli (1998) and Sucuoglu et al. (1998), and their conseqnuences on linear and bilinear SDOF system responses have been investigated in a paper by Makris and Black (2004).

In this study, the relationship between ground motion characteristics and input energy resulting from long period coherent velocity pulses produced either by a distinct acceleration pulse or a succession of high-freqnuency acceleration pulses are explored to further expand our understanding of the destructive potential of near-fault accelerograms. Additionally, simple sinusoidal pulse models to simulate forward directivity and fling effects are employed to illustrate the consequences of pulse period and pulse shape on input energy. While these preliminary evaluations are carried out based on linear SDOF systems, this paper ultimately investigates the correlation between interstory drift demands of nonlinear MDOF systems and input seismic energy computed using absolute and relative energy formulations.

2. SEISMIC INPUT ENERGY FORMULATIONS

The equation of motion of a damped SDOF system is:

$$m\ddot{u}_t + c\dot{u} + f(u) = 0 \tag{1}$$

where m is the mass, c is the damping coefficient, $f(u)$ is the restoring force. $f(u) = ku$ for material linear and nonlinear systems, and $f(u) = [k-k_G]u$ for system when P-Delta component is accounted for. The geometric stiffness matrix, $k_G = g/l$ is for unit mass system with no additional axial load (g is gravitational acceleration and l is the height of a SDOF system). u_t ($u_t = u+u_g$) is the absolute (total) displacement, u_g is the ground displacement, and u is the relative displacement of the system with respect to the ground. It is also possible to express Eqn 1 in the following form:

$$m\ddot{u} + c\dot{u} + f(u) = -m\ddot{u}_g \tag{2}$$

Integration of Eqns. 1 and 2 with respect to relative displacement u leads to two definitions of input energy. Integrating Eqn. 1 with respect to u gives the absolute energy formulation of a viscous damped SDOF system subjected to horizontal motion (see Figure 1a) as follows:

$$\begin{aligned}\frac{m[\dot{u}_g + \dot{u}]^2}{2} + \int c\dot{u}du + \int f(u)du &= \int m[\ddot{u}_g + \ddot{u}]du_g \\ &= \int m[\ddot{u}_g + \ddot{u}]\dot{u}_g dt\end{aligned} \tag{3}$$

Eqn. 3 can also be written in a general form, which identifies the different energy components:

$$E_K + E_\xi + (E_S + E_H) = E_I \tag{4}$$

where E_I is the absolute input energy, E_K is the absolute kinetic energy, E_ξ is the damping energy, E_S is the elastic strain energy and E_H is the plastic strain energy (irrecoverable hysteretic energy). As a corollary, integration of Eqn. 2 with respect to u results in the relative energy formulation of a fixed-based SDOF system as shown in Figure 1b:

$$\frac{m\dot{u}^2}{2} + \int c\dot{u}du + \int f(u)du = -\int m\ddot{u}_g du = -\int m\ddot{u}_g \dot{u}dt \tag{5}$$

Eqn. 5 can be expressed in terms of the following energy components:

$$E'_K + E_\xi + (E_S + E_H) = E'_I \tag{6}$$

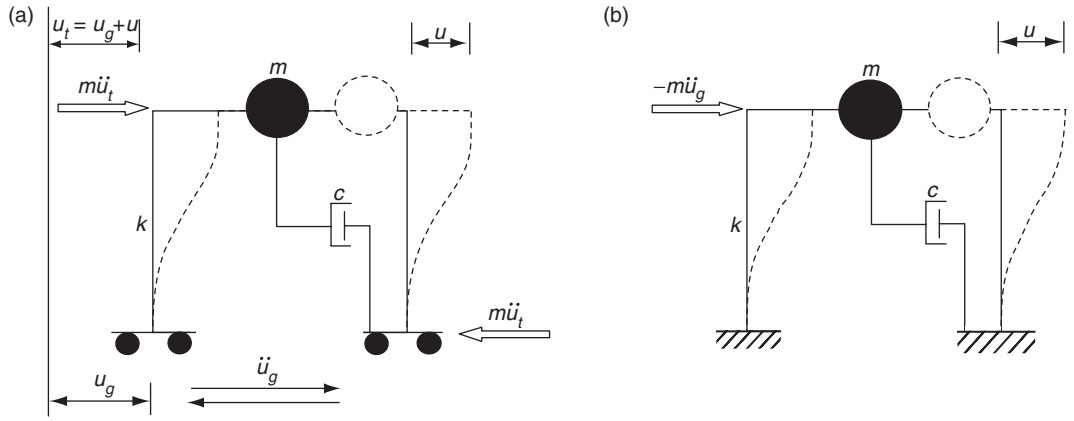

Figure 1. Idealized mathematical models of SDOF system used for (a) absolute and (b) relative energy formulations.

where E_k is the relative input energy, and E_k is the relative kinetic energy. E_I represents the work done by the inertia force ($m\ddot{u}_t$) acting on the structure, which is equivalent to the work done by the total base shear on the ground displacement. On the other hand, E_I' represents the work done on a fixed based system by an equivalent lateral force, thereby excluding rigid body translation effects. The difference between the two energy formulations is a result of the different definitions of kinetic energy (E_K' vs E_K), while damping and strain energy terms remain identical in both definitions. The difference between the two energy formulations therefore can be written as follows:

$$E_I - E_I' = E_K - E_K' = \frac{1}{2} m\dot{u}_g^2 + m\dot{u}_g \dot{u} \tag{7}$$

The right hand side of Eqn. 7 has two entities; the former is the kinetic energy (a positive quantity always) due to ground velocity ($\dot{u}_g$), while later ($m\dot{u}_g \dot{u} = m\ddot{u}_g du$) is the work done by ground acceleration ($m\ddot{u}_g$) on the respective incremental system displacement (du). This last term can take a positive or negative value depends on velocity phase difference between ground and system. In other words, if the ground velocity ($\dot{u}_g$) is out-of-phase with relative velocity of mass ($\dot{u}$), then last term in Eqn. 7 ($m\dot{u}_g \dot{u}$) becomes negative quantity. As long as it remains less than kinetic energy term $\left(\frac{1}{2} m\dot{u}_g^2\right)$, the difference between absolute and relative energy definitions remains positive. In such cases, absolute energy becomes larger than relative. However, depends on the relative velocity of mass, the negative value of last entity in Eqn. 7 may exceed the kinetic energy term, and results in larger relative energy content than that of absolute.

It is now generally well-known that absolute and relative energies tend to differ in magnitude for very flexible or very rigid systems. For flexible systems where the vibration period is significantly larger than the predominant ground motion period, the mass of the system preserves its original position while the ground moves. In this case, the absolute energy approaches zero while significant relative input energy builds up. Conversely, in case of rigid systems, the relative movement of the mass with respect to the ground is negligibly small and results in near zero relative energy, yet considerable absolute energy may develop. These conditions can easily be visualized using energy difference expression (i.e. Eqn. 7).

3. SEISMIC ENERGY INPUT TO SDOF SYSTEMS

While interpretation of far-fault strong motions during the last three decades has evolved considerably, the recent 1994 Northridge (Calif.), 1999 Chi-Chi (Taiwan) and 1999 Kocaeli and Duzce (Turkey) earthquakes uncovered significant differences between near-fault and far-fault ground motions in terms of their distinct acceleration and velocity pulses. These pulses, modified by directivity effects, originate due to the nature of the fault-slip mechanism. Velocity pulses and the characteristics of acceleration pulses that lead to the development of a coherent velocity pulse, as will be demonstrated in this paper, also play a significant role in determining the absolute and relative input energy outcomes of near-fault records and are remarkably different than those produced by far-fault records.

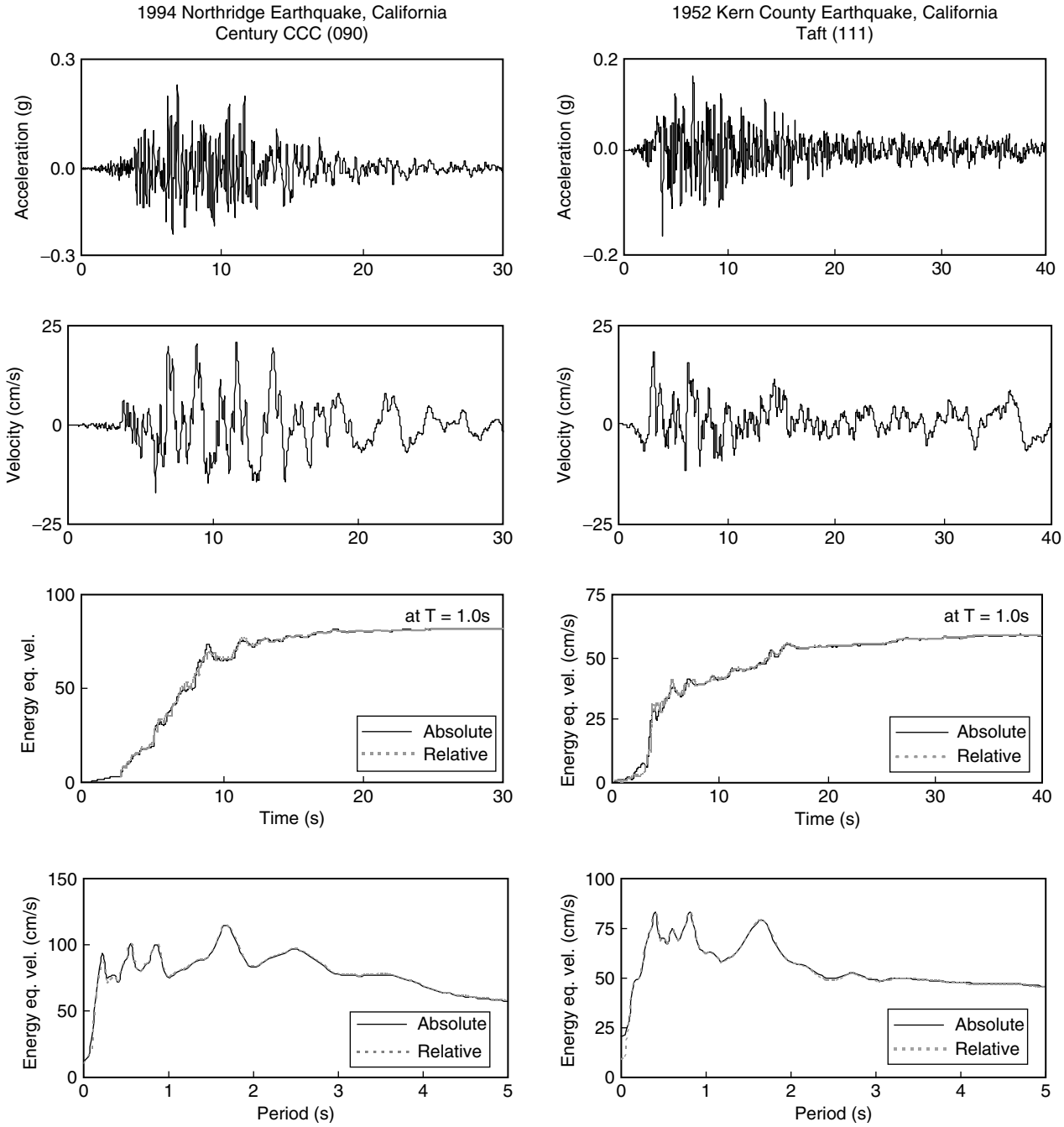

Figure 2. Acceleration, velocity and energy equivalent velocity time history plots, together with energy equivalent velocity spectra (5% damping) for typical far-fault records.

For ordinary far-fault ground motions, the input energy cumulatively increases and reaches a peak at the termination of the ground movement and this peak energy value, typically used to generate conventional input energy spectra, is similar for both relative and absolute energy measures. Figure 2 is an example of the energy response history and resultant input energy spectrum computed for ordinary far-fault records of selected components from the 1994 Northridge and 1952 Kern County earthquakes. In order to facilitate comparison between different records, the input energy is converted into an energy equivalent velocity as $V_{EQ} = \sqrt{2E_I / m}$ and $V'_{EQ} = \sqrt{2E'_I / m}$ for absolute and relative energy definitions, respectively. Henceforth, the energy equivalent velocity will be used as the measure of input energy. As portrayed in Figure 2, the two different input energy definitions result in virtually similar energy response histories and input energy spectra. Ordinary far-fault records contain typical

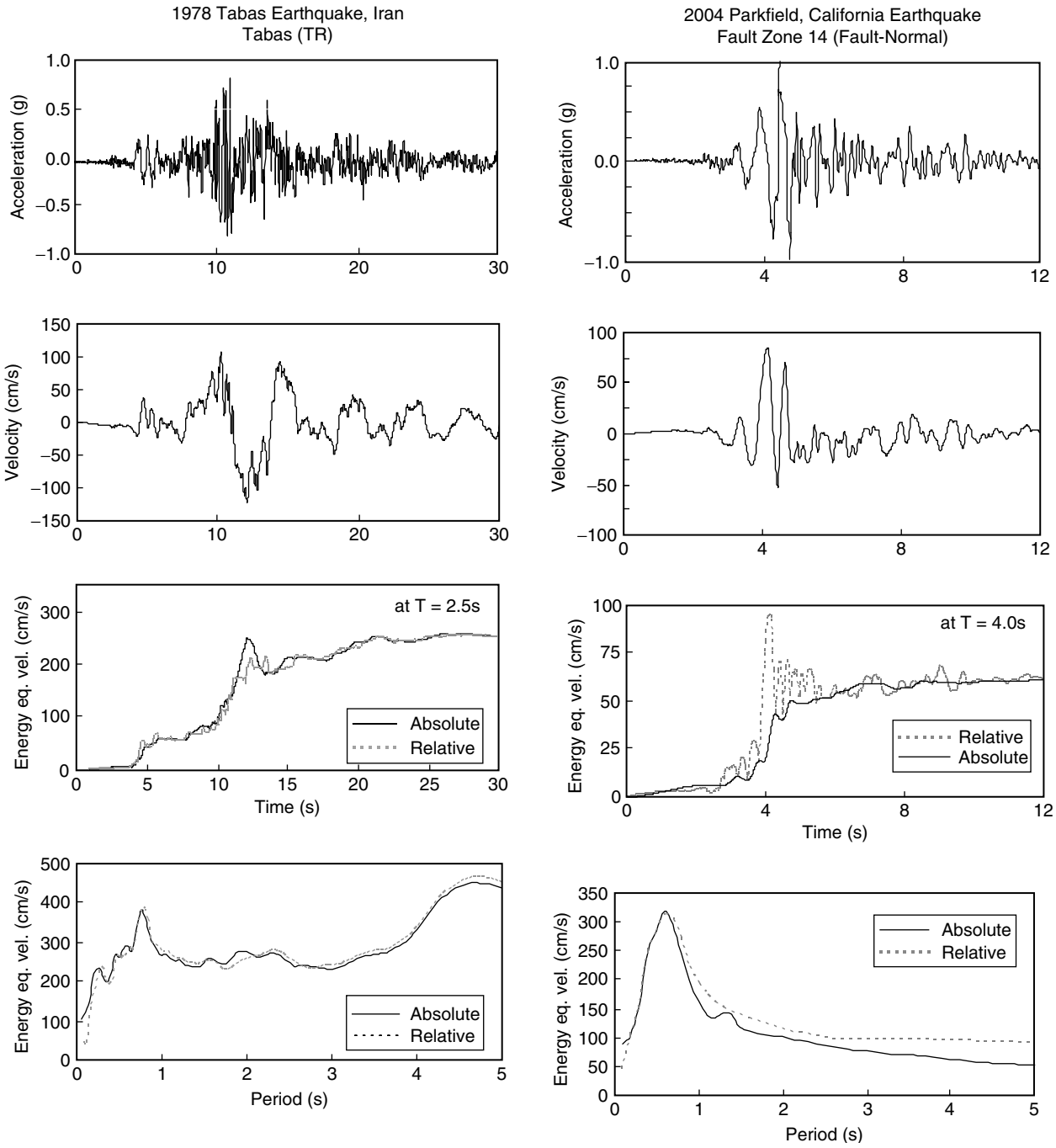

Figure 3. Acceleration, velocity and energy equivalent velocity time history plots, together with energy equivalent velocity spectra for typical near-fault forward directivity records.

random high-frequency content in the acceleration trace that result in multiple spikes in the velocity time-series. These spikes progressively increase the input energy and are associated with damage accumulation by inducing multiple inelastic deformation cycles (a low cycle fatigue phenomenon). Therefore, the number of plastic half-cycles becomes an important parameter to estimate the peak input energy. Near-fault ground motions, on the other hand, contain coherent long-period intense velocity pulses as evident in the Tabas and Fault Zone-14 stations records shown in Figure 3. These two records are characterized by forward directivity, which occurs when the fault rupture propagates with a velocity close to the shear-wave velocity. The displacement associated with such a shear-wave velocity is largest in the fault normal direction for strike-slip faults. The important distinction between the two forward directivity records displayed is the initiation of the

velocity pulses. These pulses may originate either due to succession of high frequency acceleration peaks that resemble far-fault records (as in the case of the Tabas record where the acceleration time-history is packed with high frequency spikes without a distinguishable acceleration pulse) or a distinct acceleration pulse (as in the case of the Fault Zone-14 record). This difference can influence the resultant input energy depending on whether the relative or absolute input energy definition is used. Forward directivity records without distinctive acceleration pulses have generally similar energy histories and spectra. However, the presence of a distinct acceleration pulse generates smaller or larger relative energy magnitude in the short and long period ranges, respectively, than absolute energy. It should be also noted that actual energy difference is much larger since energy equivalent velocities are compared in Figure 3. For forward-directivity records with distinguishable acceleration pulses, relative energy is generally higher than absolute energy in the long period range. Consistently similar results were obtained for a number of near-fault forward directivity records investigated for linear and nonlinear SDOF systems (Kalkan 2006; Kalkan et al. 2006).

Comparison of energy-time history of the two records elucidates another important feature of acceleration pulses. In contrast to records without a noticeable acceleration pulse wherein the input energy gradually builds up and reaches a maximum near the termination of the ground motion, records with distinct single acceleration pulses result in instantaneous energy spike(s) as an input to the system with minimal accumulation of energy afterwards. To be more specific, the difference between relative and absolute energy become largest during sudden energy spike(s). This difference is influenced by two components: (i) the kinetic energy of the ground motion (always a positive quantity) which is independent of the system response and corresponding spectral period; (ii) the incremental work done by the ground acceleration on system relative displacement which becomes a positive value only if the ground velocity is in-phase with the system relative velocity (see Eqn. 7). Hence, the difference between the two energy definitions reaches a minimum when the ground velocity remains mostly out-of-phase with the system relative velocity.

Figures 4 and 5 portray the acceleration, velocity, energy time-history, and corresponding energy-spectra of fling motions recorded during the 1999 Kocaeli (Turkey) and Chi-Chi (Taiwan) earthquakes. Fling, being a result of the evolution of residual ground displacement due to tectonic deformation associated with the rupture mechanism, is generally characterized by a unidirectional large amplitude velocity pulse and a monotonic step in the displacement time-series (Kalkan and Kunnath 2006). Fling takes place in the direction of fault slip thereby it is not strongly coupled with forward directivity. It arises in strike-slip faults in the strike parallel direction as in Kocaeli and Duzce earthquakes or in the strike-normal direction for dip-slips faults as in Chi-Chi earthquake.

The difference between forward directivity and fling records is more clearly observable in the velocity and displacement time-series. Unlike fling motions, forward directivity records are characterized by double-sided velocity pulses. Despite the difference in the velocity pulse shape, the initiation of these pulses is similar regardless of the directivity effect. As such, Sakarya and TCU074 records consist of compressed acceleration spikes, whereas in TCU052 and TCU068 records, they contain a distinct single acceleration pulse.

Figures 4 and 5 also show the energy response history and input energy spectra of fling motions computed using absolute and relative energy formulations. Sakarya and TCU074 ground motions (both of which do not contain a distinct acceleration pulse) generate absolute and relative input energy somewhat similar to each other (though occasional spikes in the absolute input energy history may be present simply by virtue of the fact that it is a near-fault fling record, as in the case of the Sakarya record). Conversely, TCU068 and TCU052 records with a dominant acceleration pulse produce significantly larger instantaneous absolute energy spikes following the dominant pulse arrival. This noticeable difference between absolute and relative energy contents is more clearly seen in the resultant input energy spectrum at different spectral periods. In fling motions, the single-sided velocity pulse due to tectonic deformation of the ground surface manifests itself in the absolute energy plot as the work done by the rigid body translation, which cannot be captured by relative input energy.

The above findings are further substantiated by examining the ratio of absolute to relative input energy for a much larger subset of records. Figure 6 presents the statistical correlation of near-fault ground motion characteristics on input energy measures. These results are based on analyses of 76 near-fault forward directivity records (in which 25 records contain a dominant acceleration pulse) and 41 near-fault fling records (in which 6 contain a distinguishable acceleration pulse). While the relevant information for these 117 records including peak-ground-acceleration (PGA), peak-ground-velocity (PGV) and peak-ground-displacement

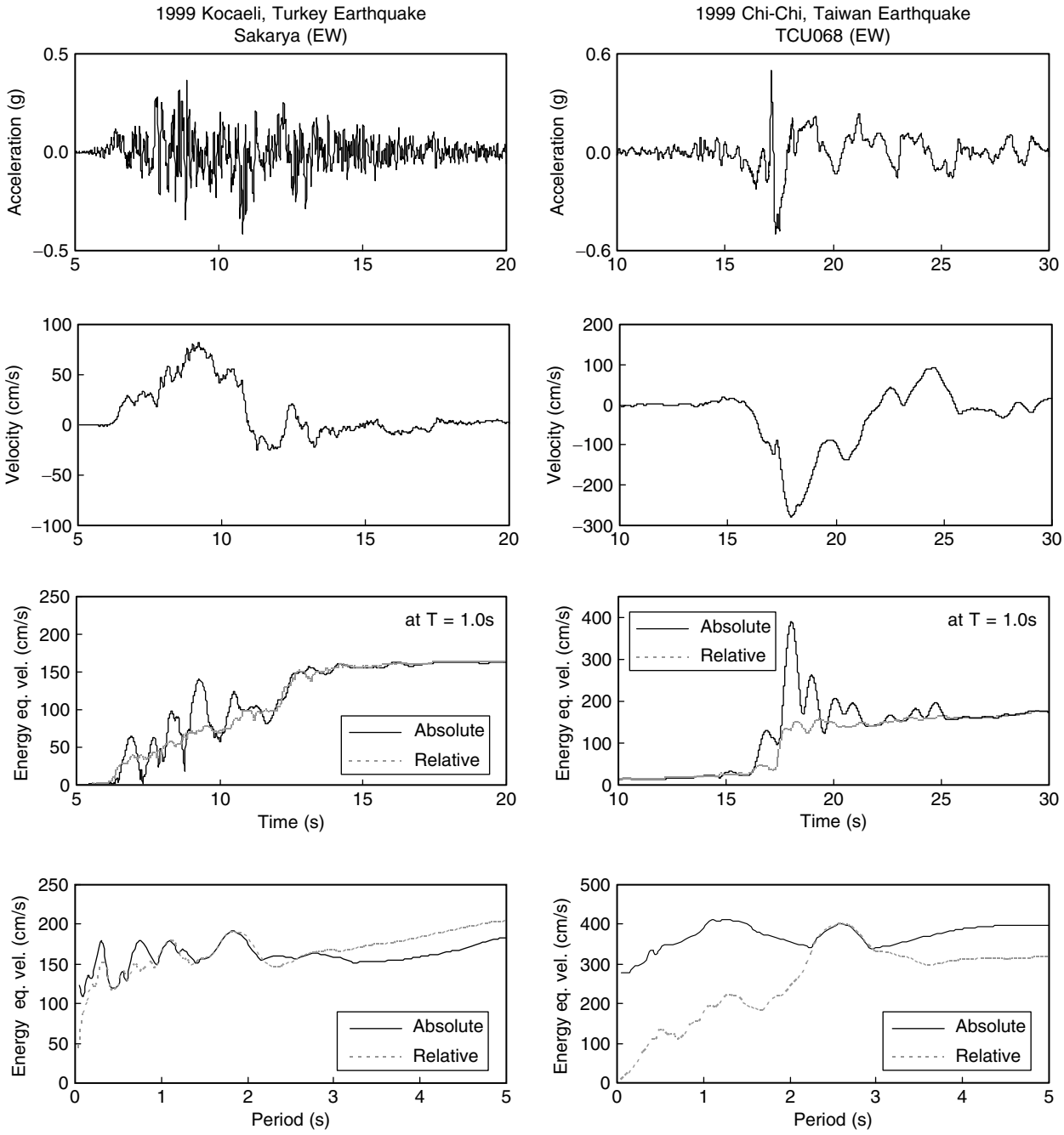

Figure 4. Acceleration, velocity and energy equivalent velocity time history plots, together with energy equivalent velocity spectra (5% damping) for typical near-fault fling records.

(PGD) are provided in Table 1A in the Appendix, the near-fault ground motion selection criteria including details of processing raw-fling motions are reported in Kalkan and Kunnath (2007). As is evident from the figure, absolute energy measures are critical in most cases with the exception of forward directivity records containing a coherent acceleration pulse wherein relative input energy is more significant.

4. SDOF ENERGY RESPONSE TO PULSE INPUTS

A practical assessment of the above issues is facilitated through the use of simple sinusoidal pulse models, wherein pulse duration and shape can be effectively varied while their collective influences on absolute and relative input energy measures and respective energy spectra can be systematically examined. Double sided

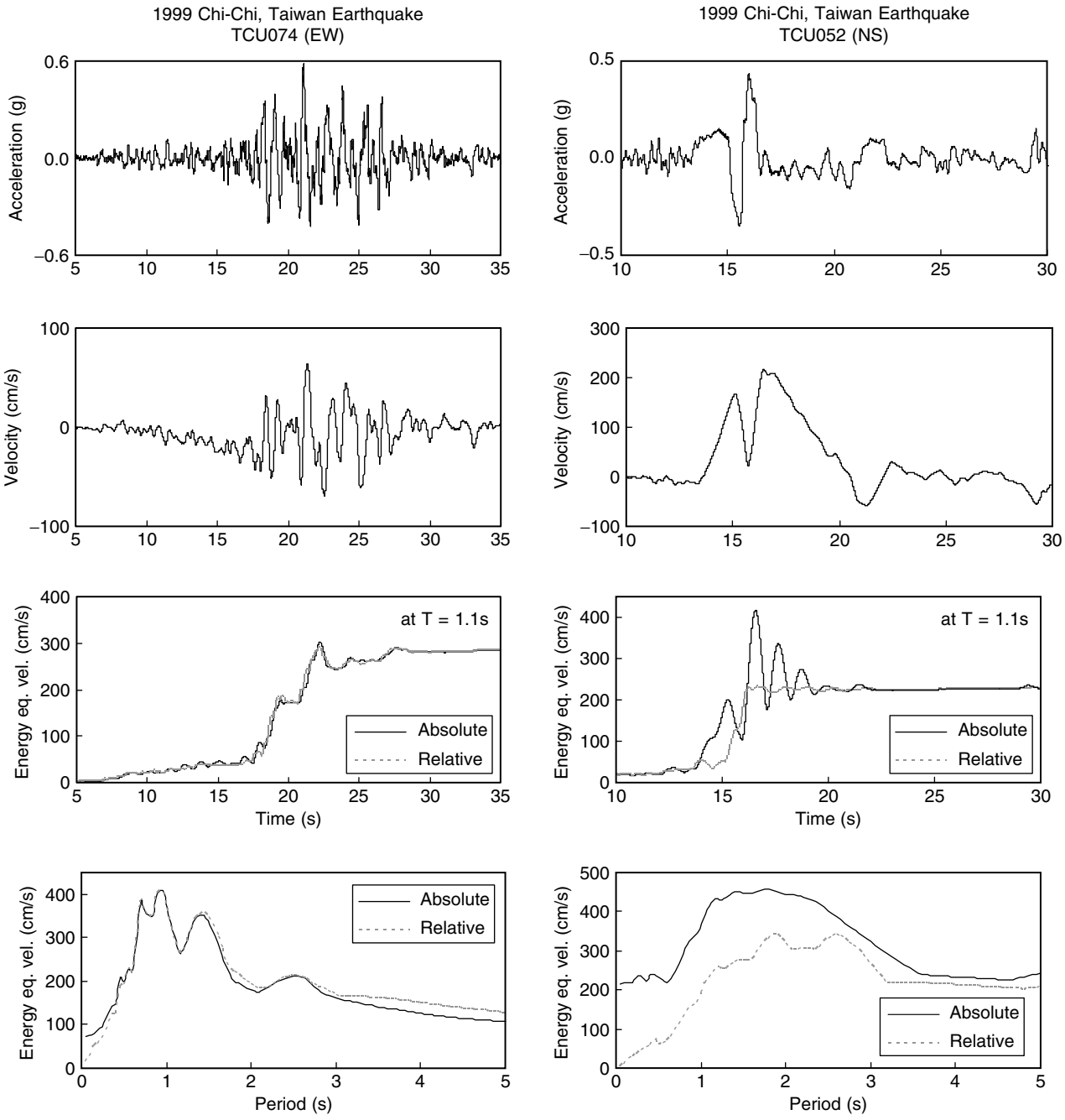

Figure 5. Acceleration, velocity and energy equivalent velocity time history plots, together with energy equivalent velocity spectra (5% damping) for additional near-fault fling records used in this study.

and unidirectional sinusoidal waveforms to represent velocity time traces are used to imitate, respectively, forward directivity and fling records as illustrated in Figure 7. The basis and formulations of these pulses are given in Kalkan and Kunnath (2006). Similar waveform models have also been utilized in many other studies (Makris and Black 2004; Sasani and Bertero 2000; Alavi and Krawinkler 2003; Mavroeidis et al. 2004), and shown to provide reasonable representation of important characteristics of impulsive near-fault accelerograms.

Figure 8 compares the equivalent velocity spectra (5% damping) of simple forward directivity and fling pulse models having pulse periods of 0.5, 1.0, 2.0 and 4.0 s computed using absolute and relative input energy formulations. All pulse records were scaled to the same PGA of 0.5 g. Comparisons of energy-spectra demonstrate that simple pulse models consistently impart larger absolute energy than relative energy for spectral periods less than the pulse period (*Tp*). Conversely, relative input energy becomes larger for periods larger than

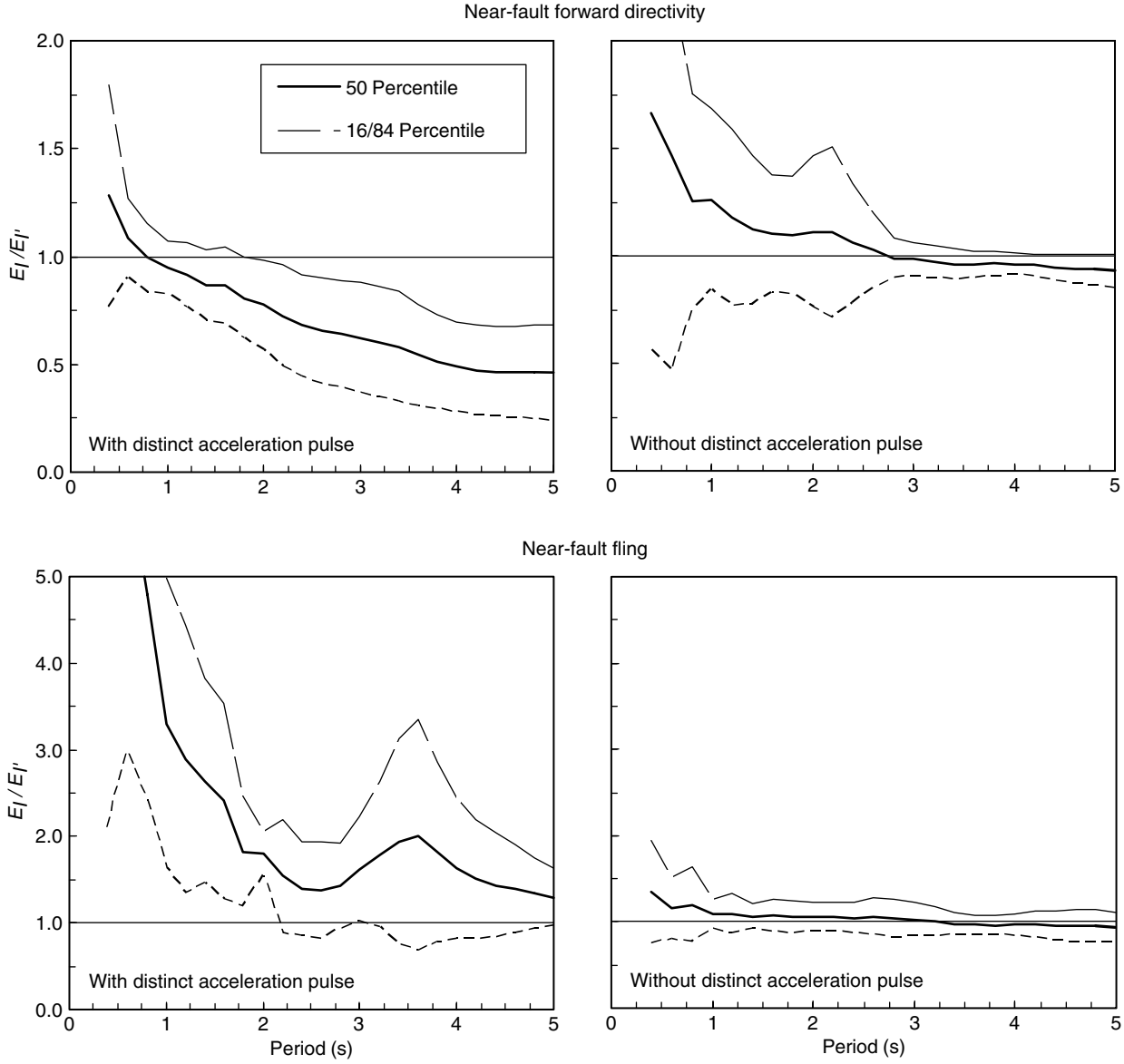

Figure 6. Mean and 16 and 84 percentiles variation of absolute (E_I) to relative energy (E_I') ratio for near-fault records with distinguishable acceleration pulses (Left) and for records with random high frequency acceleration spikes (Right).

about 2*Tp* for forward directivity and about 3*Tp* for records with fling characteristics. In the period range of *Tp* to 2*Tp* for forward directivity and *Tp* to 3*Tp* for fling, both energy notations generate similar results. As noted for real earthquakes, the difference in input energy using relative and absolute energy definitions becomes more severe in case of fling.

The vertical line in the spectra plots indicates the spectral period corresponding to pulse period. For each energy-spectrum, the peak spectral value is observed to be in the proximity of the pulse period. The shape of the energy-spectrum is significantly affected by the type of pulse and its period. Compared to forward directivity, fling models result in higher input energy in the spectrum for a wider range of spectral periods. Another influential parameter on the spectral shape is the duration of the acceleration pulse (i.e., T_{pulse}). Increase in pulse period associated with larger PGV/PGA ratio results in increased seismic energy input regardless of pulse type. Similar to real recordings (Figure 4 and 5), difference between absolute and relative energy spectrum is more pronounced in fling pulses than forward directivity pulses. This significant energy difference is attributed to higher PGV and associated kinetic energy of ground in fling motions wherein the single sided velocity pulse produces larger incremental work while being more in-phase with system relative velocity (see Eqn. 7).

Table 1 A. Near-fault ground motion dataset

No.	Year	Earthquake	M_w	Mech.1	Station	Near Fault Characteristics	Dist.[2] (km)	Site Class[3]	Data Src.[4]	Comp.	PGA (g)	PGV (cm/s)	PGD (cm)
1	1966	Parkfield	6.1	SS	Temblor	Forward-Dir.	11.4	C	1	205	0.36	21.64	3.79
2	1966	Parkfield	6.0	SS	Cholame 2WA	Forward-Dir.	6.6	C	1	065	0.48	75.04	22.37
3	1971	San Fernando	6.6	TH/REV	Pacoima Dam	Forward-Dir.	2.8	B	1	254	1.16	54.30	11.73
4	1978	Tabas	7.4	TH	Tabas	Forward-Dir.	3.0	D	1	TR	0.85	121.43	95.11
5	1979	Imperial-Valley	6.5	SS	El Centro Array #3	Forward-Dir.	13.8	D	1	140	0.27	46.84	18.90
6	1979	Imperial-Valley	6.5	SS	El Centro Diff. Array	Forward-Dir.	5.6	D	1	270	0.35	71.23	45.90
7	1979	Imperial-Valley	6.5	SS	El Centro Imp. Co. Cent.	Forward-Dir.	7.6	D	1	092	0.23	68.80	39.38
8	1979	Imperial-Valley	6.5	SS	El Centro Array #4	Forward-Dir.	8.3	D	2	S50W	0.36	80.56	72.00
9	1979	Imperial-Valley	6.5	SS	El Centro Array #6	Forward-Dir.	3.5	D	2	S50W	0.44	113.35	72.00
10	1979	Imperial-Valley	6.5	SS	El Centro Array #7	Forward-Dir.	3.1	D	2	S50W	0.46	113.30	47.46
11	1979	Imperial-Valley	6.5	SS	El Centro Array #8	Forward-Dir.	4.5	D	1	140	0.60	54.26	32.39
12	1979	Imperial-Valley	6.5	SS	El Centro Array #10	Forward-Dir.	8.7	D	2	320	0.23	46.26	26.74
13	1979	Imperial-Valley	6.5	SS	Bonds Center	Forward-Dir.	4.4	D	1	140	0.59	45.22	16.80
14	1979	Imperial-Valley	6.5	SS	Holtville Post Office	Forward-Dir.	8.8	D	1	225	0.25	48.76	31.63
15	1979	Imperial-Valley	6.5	SS	Brawley Airport	Forward-Dir.	11.3	D	1	225	0.16	35.85	22.39
16	1979	Imperial-Valley	6.5	SS	EC Meloland Overpass	Forward-Dir.	3.1	D	1	270	0.30	90.46	31.68
17	1983	Coalinga	6.5	TH/REV	Pleasant Valley P.P. Bld.	Forward-Dir.	8.5	-	1	045	0.38	32.40	6.42
18	1984	Morgan Hill	6.1	SS	Gilroy STA #2	Forward-Dir.	11.8	D	2	090	0.21	12.75	1.98
19	1984	Morgan Hill	6.1	SS	Gilroy STA #3	Forward-Dir.	10.3	D	2	090	0.19	12.23	2.58
20	1984	Morgan Hill	6.1	SS	Gilroy STA #6	Forward-Dir.	6.1	C	2	090	0.29	36.54	5.21
21	1984	Morgan Hill	6.1	SS	Coyote Lake Dam	Forward-Dir.	1.5	B	2	285	1.16	80.29	10.53
22	1984	Morgan Hill	6.1	SS	Halls Valley	Forward-Dir.	2.5	D	2	240	0.31	39.52	6.56
23	1984	Morgan Hill	6.1	SS	Anderson Dam	Forward-Dir.	4.8	B	2	340	0.29	28.00	5.75
24	1985	Nahanni-Canada	6.9	-	Site 1, Stn. 6097	Forward-Dir.	6.0	-	1	010	0.98	46.05	9.62
25	1986	N. Palm Springs	6.2	SS	Whitewater Trout Farm	Forward-Dir.	6.1	-	1	270	0.61	31.48	4.59
26	1986	N. Palm Springs	6.2	SS	Desert Hot	Forward-Dir.	6.8	D	1	000	0.33	29.46	5.70
27	1986	N. Palm Springs	6.2	SS	N. Palm Spr. Post Office	Forward-Dir.	3.6	-	1	210	0.59	73.27	11.47
28	1987	Superstition Hills	6.4	SS	Parachute Test Site	Forward-Dir.	0.7	D	1	225	0.46	111.99	52.46
29	1987	Superstition Hills	6.4	SS	El Centro Imp. Co. Cent.	Forward-Dir.	13.9	D	1	000	0.36	46.36	17.58
30	1987	Whittier-Narrows	6.1	TH/REV	LA Vernon Ave., Cmd Terminal	Forward-Dir.	15.7	D	1	083	0.15	13.14	1.43
31	1987	Whittier-Narrows	6.1	TH/REV	Bell LA Bulk Mail Center	Forward-Dir.	14.9	B	2	010	0.33	13.90	1.49
32	1987	Whittier-Narrows	6.1	TH/REV	Garvey Reservoir Abutment Bld.	Forward-Dir.	13.6	B	2	060	0.37	15.53	1.42
33	1989	Loma Prieta	7.0	OB	Gilroy Gav. Col.	Forward-Dir.	11.6	C	1	067	0.36	28.63	6.36
34	1989	Loma Prieta	7.0	OB	Los Gatos Parent Center	Forward-Dir.	3.5	C	1	000	0.56	94.81	41.13
35	1989	Loma Prieta	7.0	OB	Lexington Dam	Forward-Dir.	6.3	C	2	090	0.41	94.26	36.36
36	1989	Loma Prieta	7.0	OB	Gilroy STA #1	Forward-Dir.	2.8	B	1	090	0.47	33.96	8.09
37	1989	Loma Prieta	7.0	OB	Gilroy STA #2	Forward-Dir.	4.5	D	1	000	0.37	32.92	7.19
38	1989	Loma Prieta	7.0	OB	Gilroy STA #3	Forward-Dir.	6.3	D	1	000	0.56	35.70	8.24
39	1989	Loma Prieta	7.0	OB	Gilroy His. Bld.	Forward-Dir.	12.7	-	1	090	0.28	41.97	11.12
40	1989	Loma Prieta	7.0	OB	Saratoga Aloha Ave.	Forward-Dir.	4.1	D	2	090	0.32	44.77	27.97
41	1989	Loma Prieta	7.0	OB	Saratoga W.Valley Coll.	Forward-Dir.	13.7	-	1	000	0.26	42.45	19.51
42	1989	Loma Prieta	7.0	OB	Capitola	Forward-Dir.	8.6	D	1	000	0.53	35.03	9.17

43	1989	Loma Prieta	7.0	OB	Corralitos	Forward-Dir.	5.1	D	1	000	0.64	55.20	10.75
44	1992	Landers	7.3	SS	Lucerne Valley	Forward-Dir.	2.0	B	1	275	0.72	97.71	70.35
45	1992	Landers	7.3	SS	Joshua Tree Fire Stn.	Forward-Dir.	10.0	D	1	000	0.27	27.50	9.12
46	1992	Cape Mendocino	7.1	TH	Petrolia, General Store	Forward-Dir.	15.9	C	1	090	0.66	90.16	28.89
47	1992	Erzincan	6.7	SS	Erzincan	Forward-Dir.	2.0	C	1	EW	0.50	64.32	21.93
48	1994	Northridge	6.7	TH	Rinaldi Rec. Stn.	Forward-Dir.	8.6	D	2	S49W	0.84	174.79	33.40
49	1994	Northridge	6.7	TH	Newhall LA Fire Stn.	Forward-Dir.	7.1	D	1	090	0.58	75.63	18.91
50	1994	Northridge	6.7	TH	Newhall Pico Canyon	Forward-Dir.	7.1	D	1	316	0.33	67.44	16.11
51	1994	Northridge	6.7	TH	Jensen Filt. Plant	Forward-Dir.	6.2	D	1	022	0.42	106.30	43.25
52	1994	Northridge	6.7	TH	Sepulveda Va. Hospital	Forward-Dir.	9.5	D	1	360	0.94	75.92	15.10
53	1994	Northridge	6.7	TH	Pacoima Kagel Canyon	Forward-Dir.	10.6	B	1	360	0.43	51.57	8.19
54	1994	Northridge	6.7	TH	Canoga Park TC	Forward-Dir.	15.7	D	1	196	0.42	60.73	20.30
55	1994	Northridge	6.7	TH	Arieta Nordhoff Ave. Fire Stn.	Forward-Dir.	9.5	D	1	090	0.34	40.66	15.07
56	1994	Northridge	6.7	TH	Los Angeles Dam	Forward-Dir.	2.6	-	1	064	0.51	63.70	21.26
57	1994	Northridge	6.7	TH	Sylmar Olive View Hospital	Forward-Dir.	6.4	D	1	360	0.84	130.37	31.72
58	1994	Northridge	6.7	TH	Slymar Converter Sta.	Forward-Dir.	6.2	D	1	142	0.90	102.20	45.11
59	1994	Northridge	6.7	TH	Slymar Converter Sta East	Forward-Dir.	6.1	D	1	018	0.83	117.51	34.47
60	1995	Kobe	6.9	SS	Takatori	Forward-Dir.	4.3	D	1	090	0.62	120.78	32.75
61	1995	Kobe	6.9	SS	KJMA	Forward-Dir.	0.6	C	1	000	0.82	81.62	17.71
62	1999	Kocaeli	7.4	SS	Darica	Forward-Dir.	17.0	C	3	EW	0.14	45.06	66.09
63	1999	Kocaeli	7.4	SS	Duzce	Forward-Dir.	11.0	D	1	180	0.31	58.85	44.10
64	1999	Kocaeli	7.4	SS	Gebze	Forward-Dir.	15.0	B	1	000	0.24	50.30	42.69
65	1999	Duzce	7.2	SS	Bolu	Forward-Dir.	20.4	D	1	EW	0.82	62.13	13.57
66	2004	Bingol	6.4	SS	Bingol	Forward-Dir.	6.1	D	3	NS	0.56	14.65	9.82
67	2004	Parkfield	6.4	SS	Cholame IE	Forward-Dir.	6.5	D	5	FN	0.47	53.10	12.83
68	2004	Parkfield	6.4	SS	Cholame 4AW	Forward-Dir.	8.4	D	5	FN	0.19	22.16	7.77
69	2004	Parkfield	6.4	SS	Cholame 5W (Sta 5)	Forward-Dir.	10.0	D	5	FN	0.21	17.38	2.41
70	2004	Parkfield	6.4	SS	Cholame 6W	Forward-Dir.	10.0	D	5	FN	0.41	19.64	4.17
71	2004	Parkfield	6.4	SS	Fault Zone 1	Forward-Dir.	3.4	D	5	FN	0.50	64.15	12.64
72	2004	Parkfield	6.4	SS	Cholame 3W	Forward-Dir.	7.2	D	5	FN	0.44	45.00	10.39
73	2004	Parkfield	6.4	SS	Cholame 4W	Forward-Dir.	7.5	C	5	FN	0.57	38.37	5.30
74	2004	Parkfield	6.4	SS	Cholame 2W	Forward-Dir.	6.7	D	5	FN	0.46	49.98	14.54
75	2004	Parkfield	6.4	SS	Cholame 2E	Forward-Dir.	7.3	C	5	FN	0.34	23.67	2.82
76	2004	Parkfield	6.4	SS	Cholame 3E	Forward-Dir.	7.6	C	5	FN	0.65	34.40	5.56
77	1999	Chi-Chi	7.6	TH	TCU052	Fling	1.8	D	4	EW	0.35	178.00	493.52
78	1999	Chi-Chi	7.6	TH	TCU052	Fling	1.8	D	4	NS	0.44	216.00	709.09
79	1999	Chi-Chi	7.6	TH	TCU068	Fling	3.0	D	4	EW	0.50	277.56	715.82
80	1999	Chi-Chi	7.6	TH	TCU068	Fling	3.0	D	4	NS	0.36	294.14	895.72
81	1999	Chi-Chi	7.6	TH	TCU074	Fling	13.8	D	4	EW	0.59	68.90	193.22
82	1999	Chi-Chi	7.6	TH	TCU074	Fling	13.8	D	4	NS	0.37	47.95	155.41
83	1999	Chi-Chi	7.6	TH	TCU084	Fling	11.4	C	4	EW	0.98	140.43	204.59
84	1999	Chi-Chi	7.6	TH	TCU084	Fling	11.4	C	4	NS	0.42	42.63	64.91
85	1999	Chi-Chi	7.6	TH	TCU129	Fling	2.2	D	4	EW	0.98	66.92	126.13

(Continued)

Table 1 A (*continued*)

No.	Year	Earthquake	M_w	Mech.[1]	Station	Near Fault Characteristics	Dist.[2] (km)	Site Class[3]	Data Src.	Comp.	PGA (g)	PGV (cm/s)	PGD (cm)
86	1999	Chi-Chi	7.6	TH	TCU129	Fling	2.2	D	4	NS	0.61	54.56	82.70
87	1999	Kocaeli	7.4	SS	Yarmica	Fling	3.3	D	3	EW	0.23	88.83	184.84
88	1999	Kocaeli	7.4	SS	Yarmica	Fling	3.3	D	3	NS	0.33	88.38	152.12
89	1999	Kocaeli	7.4	SS	Lzmit	Fling	4.3	B	3	NS	0.17	27.19	23.67
90	1999	Kocaeli	7.4	SS	Lzmit	Fling	4.3	B	3	EW	0.23	48.87	95.49
91	1999	Kocaeli	7.4	SS	Sakarya	Fling	3.2	C	3	EW	0.41	82.05	205.93
92	1999	Chi-Chi	7.6	TH	TCU102	Fling	1.2	D	4	NS	0.17	68.62	83.78
93	1999	Chi-Chi	7.6	TH	TCU102	Fling	1.2	D	4	EW	0.29	84.52	153.88
94	1999	Chi-Chi	7.6	TH	TCU089	Fling	8.3	C	4	NS	0.22	33.92	141.33
95	1999	Chi-Chi	7.6	TH	TCU089	Fling	8.3	C	4	EW	0.34	44.43	193.90
96	1999	Chi-Chi	7.6	TH	TCU049	Fling	3.3	D	4	NS	0.24	57.49	102.66
97	1999	Chi-Chi	7.6	TH	TCU049	Fling	3.3	D	4	EW	0.27	54.79	121.77
98	1999	Chi-Chi	7.6	TH	TCU067	Fling	1.1	D	4	NS	0.31	53.47	103.20
99	1999	Chi-Chi	7.6	TH	TCU067	Fling	1.1	D	4	EW	0.48	94.31	181.25
100	1999	Chi-Chi	7.6	TH	TCU075	Fling	3.4	D	4	NS	0.25	36.17	108.54
101	1999	Chi-Chi	7.6	TH	TCU075	Fling	3.4	D	4	EW	0.32	111.79	165.36
102	1999	Chi-Chi	7.6	TH	TCU076	Fling	3.2	D	4	NS	0.41	61.76	73.06
103	1999	Chi-Chi	7.6	TH	TCU076	Fling	3.2	D	4	EW	0.33	65.93	101.65
104	1999	Chi-Chi	7.6	TH	TCU072	Fling	7.9	D	4	NS	0.36	66.73	245.30
105	1999	Chi-Chi	7.6	TH	TCU072	Fling	7.9	D	4	EW	0.46	83.60	209.67
106	1999	Chi-Chi	7.6	TH	TCU065	Fling	2.5	D	4	NS	0.55	86.37	124.68
107	1999	Chi-Chi	7.6	TH	TCU065	Fling	2.5	D	4	EW	0.76	128.32	228.41
108	1999	Chi-Chi	7.6	TH	TCU079	Fling	11.0	D	4	NS	0.41	30.41	83.05
109	1999	Chi-Chi	7.6	TH	TCU079	Fling	11.0	D	4	EW	0.57	68.06	166.10
110	1999	Chi-Chi	7.6	TH	TCU078	Fling	8.3	D	4	NS	0.30	30.89	106.67
111	1999	Chi-Chi	7.6	TH	TCU078	Fling	8.3	D	4	EW	0.43	41.88	121.23
112	1999	Chi-Chi	7.6	TH	TCU082	Fling	4.5	D	4	NS	0.18	38.77	105.74
113	1999	Chi-Chi	7.6	TH	TCU082	Fling	4.5	D	4	EW	0.22	50.49	142.78
114	1999	Chi-Chi	7.6	TH	TCU128	Fling	9.1	C	4	NS	0.16	59.74	88.13
115	1999	Chi-Chi	7.6	TH	TCU128	Fling	9.1	C	4	EW	0.14	59.42	91.05
116	1999	Chi-Chi	7.6	TH	TCU071	Fling	4.9	D	4	NS	0.63	79.11	244.05
117	1999	Chi-Chi	7.6	TH	TCU071	Fling	4.9	D	4	EW	0.51	69.91	196.85

[1]Faulting Mechanism = TH: Thrust; REV: Reverse; SS: Strike-slip; OB: Oblique

[2]Closest distance to fault rupture (i.e., r_{jb})

[3]NEHRP Site Classifications => (B for V_S = 760 to 1500 m/s), (C for V_S = 360 to 760 m/s), (D for V_S = 180 to 360 m/s)

[4]Data Sources = 1: PEER (http://peer.berkeley.edu/smcat); 2: Cosmos (http://db.cosmos-eq.org);
3: ERD (http://angora.deprem.gov.tr/); 4: http://scman.cwb.gov.tw/eqv5/special/19990921/pgadata-asci0704.htm
5: CSMIP (http://www.quake.ca.gov/cisn-edc/idr/Parkfield_28Sep2004/idr_dist.htm)

Note: Original fling ground motions from data sources (3) and (4) were baseline corrected after removal of pre-event mean (*see* Kalkan and Kunnath 2006a)

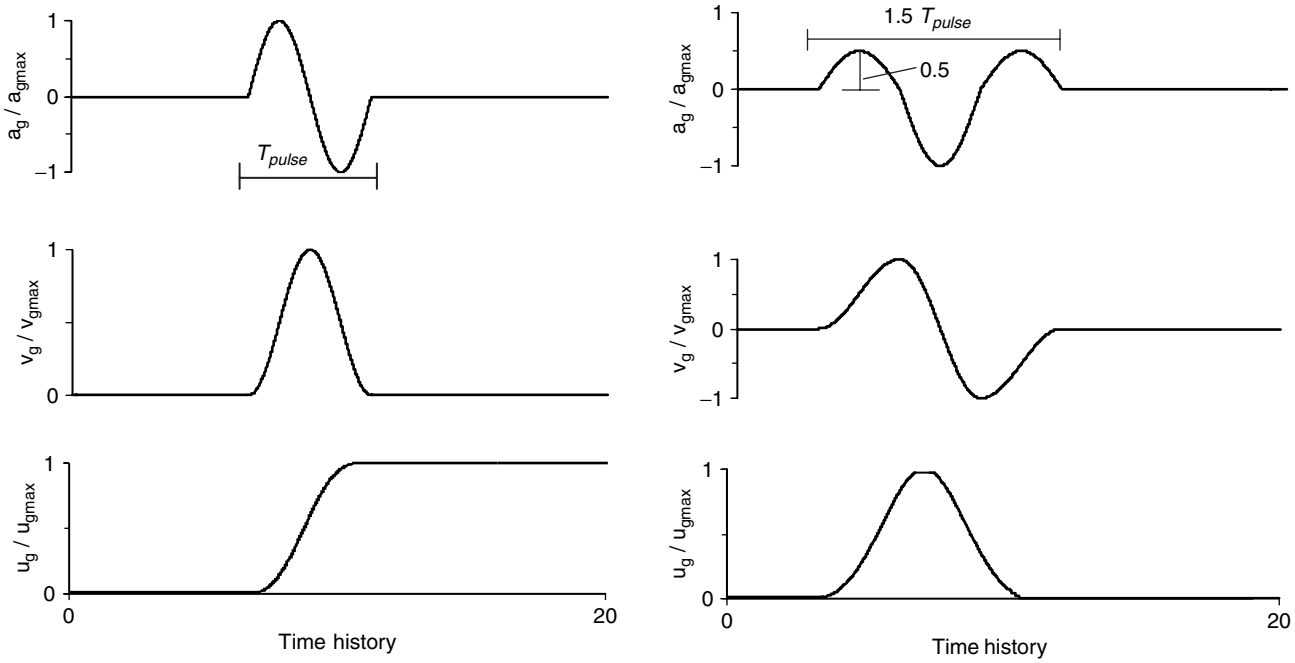

Figure 7. Sinusoidal waveforms to simulate near-fault fling pulse (Left) forward directivity pulse (Right).

5. SEISMIC ENERGY INPUT TO MDOF SYSTEMS

The general form of the absolute input energy for SDOF systems defined in Eqn 2 was expanded by Uang and Bertero to a multi-degree-of-freedom (MDOF) *N*-story system as follows:

$$\frac{1}{2}\dot{\boldsymbol{u}}_t^T \boldsymbol{m}\dot{\boldsymbol{u}}_t + \int \dot{\boldsymbol{u}}^T \boldsymbol{c}\,d\boldsymbol{u} + \int \boldsymbol{f}_s^T d\boldsymbol{u} = \int \left(\sum_{j=1}^{N} m_j \ddot{u}_{t(j)} \right) du_g = \int \left(\sum_{j=1}^{N} \boldsymbol{m}_j \ddot{\boldsymbol{u}}_{t(j)} \right) \dot{\boldsymbol{u}}_g dt \tag{11}$$

where $\boldsymbol{m}$ is the diagonal mass matrix, $\boldsymbol{c}$ is the damping matrix and $\boldsymbol{u}$ is the story relative displacement vector. Accordingly, $\boldsymbol{m}_j$ is the lumped mass of the j^{th} story and $\ddot{\boldsymbol{u}}_{t(j)}$ is the absolute (total) acceleration recorded at the j^{th} story, and N is the number of story. In the above expression, absolute energy (E_I) corresponds to the total work done due to the sum of inertia forces ($m_j \ddot{u}_{t(j)}$) at each storey level for a given ground displacement u_g at the foundation level (see Figure 9a). By the same token, it is possible to express the relative energy imparted to a MDOF system (Figure 9b) as:

$$\frac{1}{2}\dot{\boldsymbol{u}}^T \boldsymbol{m}\dot{\boldsymbol{u}} + \int \dot{\boldsymbol{u}}\boldsymbol{c}\,d\boldsymbol{u} + \int \boldsymbol{f}_s\, d\boldsymbol{u} = -\int \boldsymbol{m}\ddot{\boldsymbol{u}}_g d\boldsymbol{u} = -\int \left(\sum_{j=1}^{N} m_j \ddot{u}_g \dot{u}_j \right) dt \tag{12}$$

The difference between the absolute and relative energy formulation (Eqns. 11 and 12) for a MDOF system is essentially the difference in the kinetic energy terms, which can be expressed as

$$E_I - E_I^{'} = \frac{1}{2} m \dot{u}_g^2 + \sum_{j=1}^{N} m_j \dot{u}_g \dot{u}_{(j)} \tag{13}$$

Similar to Eqn. 7, the right side of Eqn. 13 constitutes the kinetic energy (a positive quantity always) due to ground velocity and total work done (positive or negative depends on velocity phase difference) by ground acceleration ($m_j \ddot{u}_g$) on respective incremental story displacement (du_j), where j stands for the story number.

5.1. Input Energy and Damage Potential of Near Fault Ground Motions

In this section, the correlation between damage potential of near-fault ground motions and their input energy contents are examined using the nonlinear response of two real buildings. Analytical models of instrumented 6-story and 13-story steel moment-frame buildings were created and calibrated to recorded data. Stable hysteretic models with kinematic-strain hardening were utilized. Further details of the building models including calibration studies are reported in Kunnath et al. (2004) and Kalkan (2006). Table 1 summarizes the predominant vibration properties of buildings.

The buildings were subjected to a variety of near-fault recordings having forward directivity and fling effects in

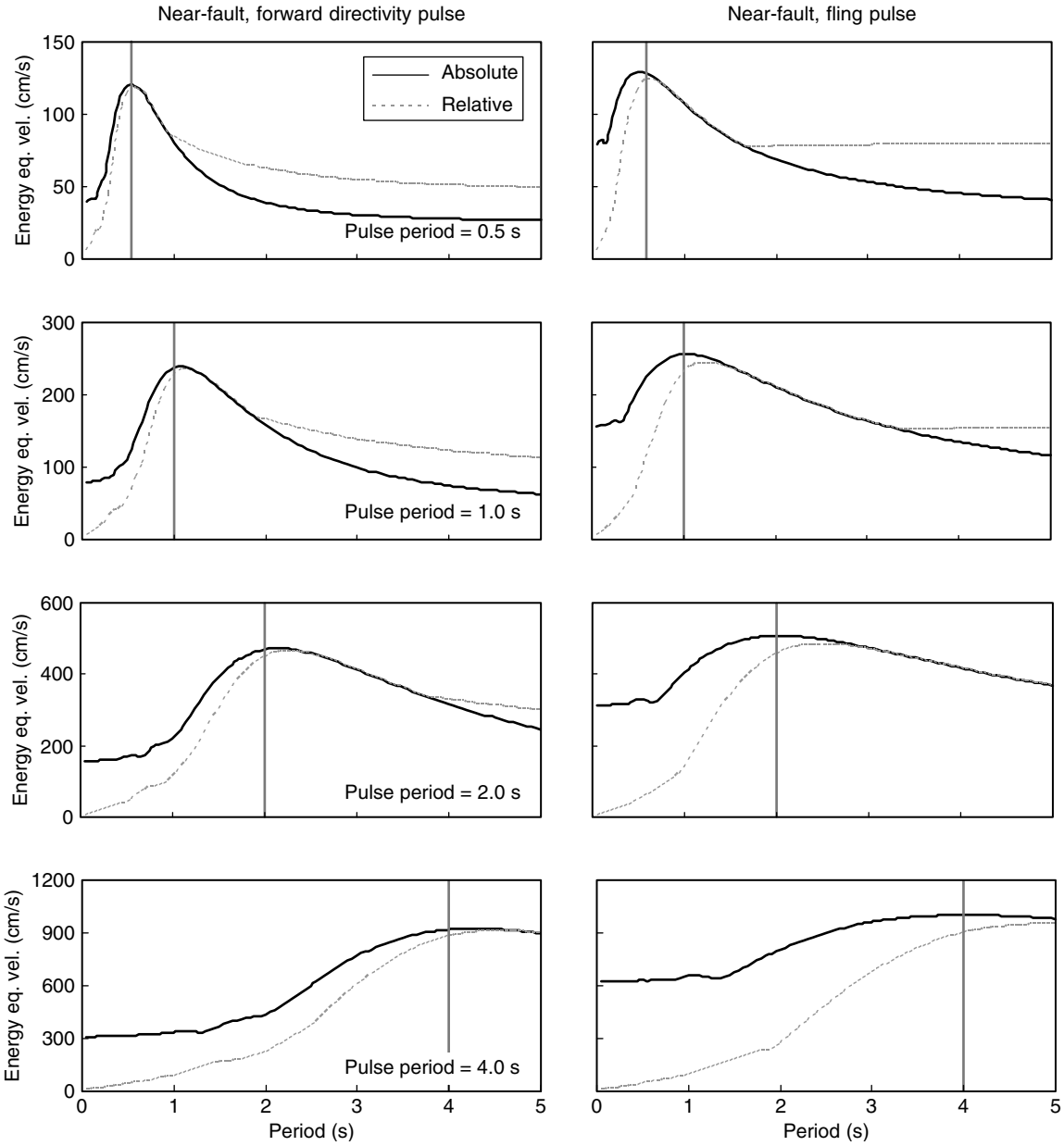

Figure 8. Comparison of energy equivalent velocity spectra (5% damping) computed using absolute and relative energy formulations for forward directivity (Left) and fling (Right) pulse models (*Vertical line in energy spectra indicates the pulse period*).

Table 1. Elastic vibration periods (in seconds) of buildings

	1st Mode	2nd Mode	3rd Mode
6-Story Steel	1.40	0.51	0.30
13-Story Steel	3.03	1.08	0.65

an effort to investigate the correlation between two input energy measures and nonlinear seismic demands. Accordingly, Figure 10 shows the peak interstory drift profiles along with the relative and absolute energy time history responses of the 6-story building subjected to two representative fling records. Recall that the TCU052 record contains a distinguishable acceleration pulse in contrast to TCU074, which does not. Since the pulse period matches the first mode period of the building (see Table 1), the TCU052 record triggers a primarily first-mode response resulting in accumulation of damage at the first story level, whereas the TCU074 record (wherein the input energy gradually accumulates over an interval of almost 11 sec) activates higher mode effects and results in larger story drifts at the fifth story level. Much of the energy in TCU052 is imparted in a short

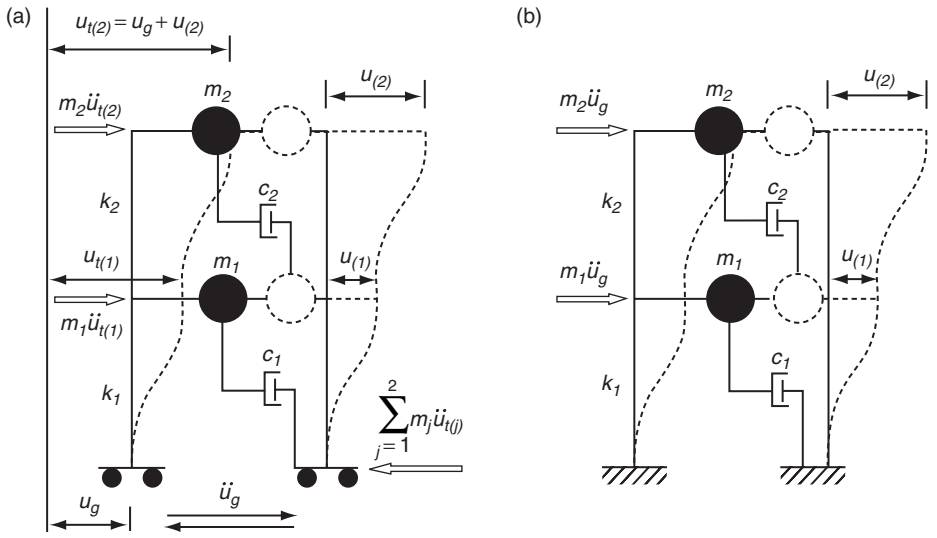

Figure 9. Idealized mathematical models of MDOF system used for (a) absolute and (b) relative energy formulations.

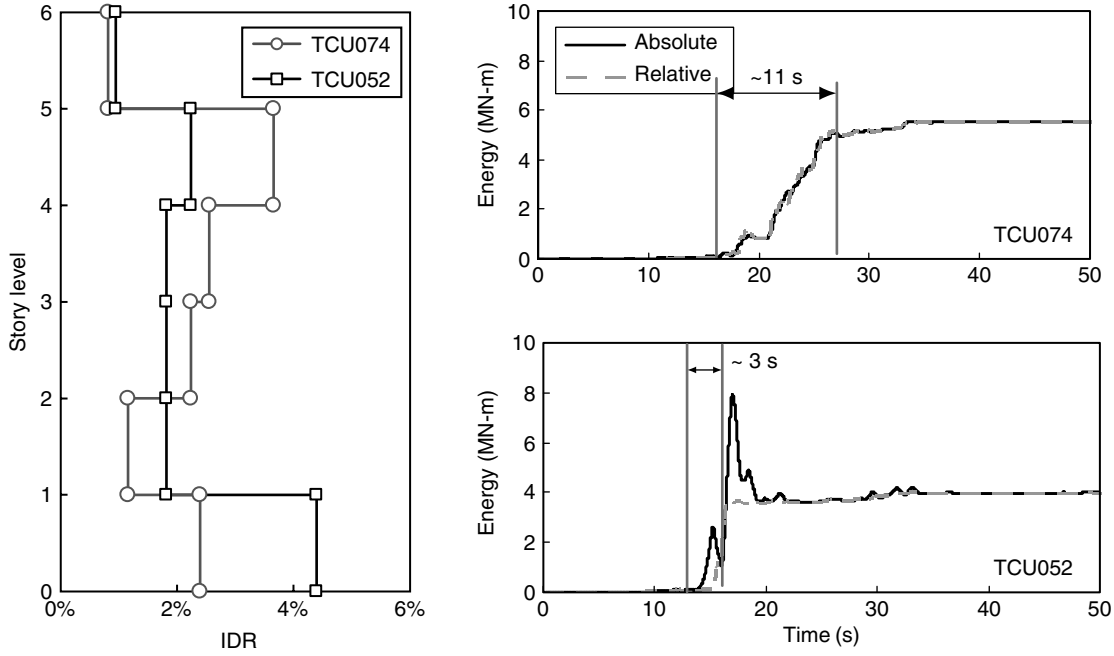

Figure 10. Peak interstory drift ratio (Left) and energy time history (Right) computed for 6-story building subjected to fling records of TCU074 and TCU052.

duration (approximately 3 sec), which appears to be another contributing factor in limiting higher mode contributions since the predominant pulse period is outside the range of the higher mode periods of the building. These results are consistent with observations of Uang and Bertero on the significance of absolute input energy measures over relative input energy in estimating the damage potential of the records. In the present study, this observation is further substantiated by examining the characteristics of the near fault records, viz. the presence of a dominant acceleration pulse and the proximity of the pulse period to the vibration period of the structure.

A very different scenario emerges for the response of the 13-story building presented in Figure 11. This building was subjected to the forward directivity records of Rinaldi Receiver Station and Tabas. Note that the former record contains a distinguishable acceleration pulse that is absent in the latter. In this case, the Rinaldi

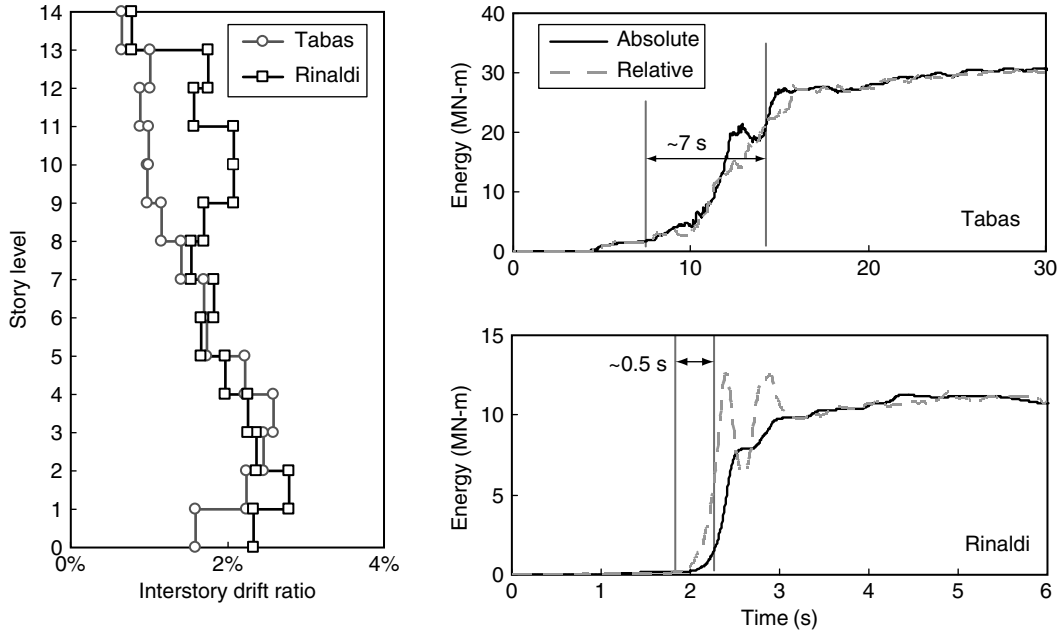

Figure 11. Peak interstory drift ratio (Left) and energy time history (Right) computed for 13-story building subjected to forward directivity records of Tabas and Rinaldi.

record produces significant demands in the upper levels while the Tabas record creates higher demand in the lower levels. Despite the fact that the Tabas record imposed significantly larger energy over a longer duration, the fact that the relative input energy reaches its peak value in a much shorter period of time is more indicative of the damage potential of the Rinaldi record as apparent from the resultant interstory drift profile. Additionally, the pulse period of the Rinaldi record is closer to the second mode period of the building. Findings presented in Figure 10 and 11 were not limited to records selected, yet representative results of comprehensive nonlinear-time-history analyses conducted on two MDOF systems.

To summarize the above findings, energy demand manifests itself either in the relative or absolute energy content depending on the dominant pulse period of the near-fault ground motion, the characteristics of the acceleration pulses and the vibration periods of the structural system. But most importantly, the sudden spikes in the input energy history (relative or absolute) are indicators of the severity of near-fault records. Therefore, important information may be overlooked if one arbitrarily uses relative or absolute energy definitions for near-fault accelerograms without carefully examining the pulse content of records.

6. CONCLUSIONS

This paper examines the fundamental principles and consequences of two commonly used energy measures using SDOF and MDOF systems subjected to far-fault and near-fault ground motions. For far-fault records, energy accumulates gradually over the duration of record and both relative and absolute energy definitions yield analogous results. In contrast, the difference between relative and absolute energy can be considerable for near-fault records. The energy difference is a function of three primary parameters (i) the characteristics of the acceleration pulses that lead to the initiation and build up of the velocity pulse, (ii) pulse period and lastly (iii) pulse shape. Velocity pulses are convolved either as a result of a succession of high frequency acceleration peaks (resembling ordinary far-fault records) or a dominant and distinctive acceleration pulse(s). For the records without an apparent acceleration pulse, both notions of input energy yield similar results. On the other hand, distinctive acceleration pulses have a significant impact on the absolute or relative energy imparted to a structural system. Records containing such acceleration pulses produce abrupt energy spike(s) in the early phase of response and are significantly larger than the energy accumulated at the termination of the ground movement.

While absolute energy is commonly accepted as representative of seismic input energy, it is established herein that it may yield misleading results in case of forward directivity near-fault records that contain a distinguishable acceleration pulse. For such records, relative input energy (which depends on the ratio of the dominant pulse period to the system fundamental period) is shown to be more meaningful energy measure.

Based on the study employing simple pulse models, peak relative energy becomes larger than peak absolute energy for periods larger than $2Tp$ for forward directivity and larger than $3Tp$ for records containing fling effects. Both measures of input energy produce similar demands in the period range from Tp to $2Tp$ for forward directivity and Tp to $3Tp$ for fling records. The amplitudes of energy spikes (i.e., difference between the two energy measures) become minimal for the system whose fundamental period is close to the dominant pulse period. Interestingly, the minimum discrepancy between the two energy terms occurs only if the sign of work done by the ground acceleration on the respective incremental system displacement becomes negative and its amplitude is close to the kinetic energy due to ground movement. This condition is possible only if the system velocity remains mostly out-of-phase with respect to ground velocity, meaning that the system tends to move in the opposite direction with respect to the ground movement.

Finally, this paper provides supporting data on the response of realistic systems subjected to the near-fault records, which reveals that the relationship between seismic demand and the two definitions of input energy depends on the dominant pulse period and the vibration properties of the system. It should be noted that linear SDOF oscillators were used in the first phase of the study reported here. Separate studies conducted on isoductile nonlinear oscillators essentially yielded similar findings but are not included herein (see Kalkan and Kunnath 2007 for details). In addition, the influence of soil-structure-interaction and associated rocking response, as well as P-Delta and coupling effects of orthogonal components of ground motions on resultant input energy were not considered in this paper, though they are part of our ongoing research.

ACKNOWLEDGMENT

Funding for this study provided by the National Science Foundation under Grant CMS-0296210, as part of the US-Japan Cooperative Program on Urban Earthquake Disaster Mitigation, is gratefully acknowledged. Any opinions, findings, and conclusions or recommendations expressed in this material are those of the authors and do not necessarily reflect the views of the National Science Foundation or the California Geological Survey where the first author is currently employed.

REFERENCES

Alavi, B. and Krawinkler, H. (2004). "Behavior of moment resisting frame structures subjected to near-fault ground motions", *Earthquake Engineering and Structural Dynamics*, Vol. 33, No. 6, pp. 687–706.

Amiri, G. G. and Dana, F. M. (2005). "Introduction of the most suitable parameter for selection of critical earthquake", *Computers & Structures*, Vol. 83, No. 8–9, pp. 613–626.

Berg, G. V. and Thomaides, S. S. (1960). "Energy consumption by structures in strong-motion earthquakes", *Proceedings of the 2nd World Conerence. on Earthquake Engineering*, Tokyo, Japan, Vol. 2, pp. 681–696.

Bertero, V. V. (1976). "Establishment of design earthquakes—Evaluation of present methods", *Proceedings of International. Symposium on Earthquake Structure Engineering*, St. Louis, Vol. 1, pp. 551–580.

Bonelli, PC. (1998). "Long seismic velocity pulses effect and damage", *Proceedings of Structural Engineering World Congress (SEWC'98)*, San Francisco.

Decanini, L. D. and Mollaioli, F. (2001). "An energy-based methodology for the assessment of seismic demand", *Soil Dynamics and Earthquake Engineering*, Vol. 21, No. 2, pp. 113–137.

Fajfar, P. and Vidic, T. (1994). "Consistent inelastic design spectra: hysteretic and input energy", *Earthquake Engineering and Structural Dynamics,* Vol. 23, pp. 523–537.

Chai, R. Y. H. and Fajfar, P. A. (2000). "procedure for estimating input energy spectra for seismic design", *Journal of Earthquake Engineering*, Vol. 4, No. 4. pp. 539–561.

Chapman, M. C. (1999). "On the use of elastic input energy for seismic hazard analysis", *Earthquake Spectra*, Vol. 15, No. 4, pp. 607–635.

Chou, C. C. and Uang, C. M. (2000). "Establishing absorbed energy spectra-an attenuation approach", *Earthquake Engineering and Structural Dynamics*, Vol. 29, pp. 1441–1455.

Chou, C. C. and Uang, C. M. "A procedure for evaluation of seismic energy demand of framed structures", *Earthquake Engineering and Structural Dynamic*s, Vol. 32, pp. 229–244.

Goel, S. C. and Berg, G. V. "Inelastic earthquake response of tall steel frames", *Journal of Structure Division* ASCE, Vol. 94, pp. 1907–1934.

Hall, J. F., Heaton, T. H., Halling, M. W. and Wald, D. J. (1995). "Near-source ground motion and its effects on flexible buildings", *Earthquake Spectra*, Vol. 11, No. 4, pp. 569–605.

Heaton, T. H., Hall, J. F., Wald, D. J. and Halling, M. W. (1995). "Response of high-rise and base-isolated buildings to a hypothetical MW 7.0 blind thrust earthquake", *Science*, Vol. 267, pp. 206–211.

Housner, G. W. (1956). "Limit design of structures to resist earthquakes", Proceedings *of the 1st World Conference on Earthquake Engineering*, Berkeley Calif.

Iwan, W. D. (1997). Drift spectrum: measure of demand for earthquake ground motions. *Journal of. Strucural Engineering,* ASCE, Vol. 123, No. 4, pp. 397–404.

Krawinkler, H. (1987). Performance assessment of steel components. *Earthquake Spectra*, Vol. 3, pp. 27–41.

Kalkan, E. (2006). *Prediction of Seismic Demands in Building Structures*. Ph.D. Dissertation, University of California at Davis (Available at http://www.geocities.com/ekalkan76).

Kalkan, E. and Kunnath, S. K. 2006, "Effects of fling-step and forward directivity on the seismic response of buildings", *Earthquake Spectra*, Vol. 22, No. 2, pp. 367–390.

Kalkan, E. and Kunnath, S. K. (2007). "Effective cyclic energy as a measure of seismic demand", *Journal of Earthquake Engineering*, Vol. 11, No. 5, pp. 725–751.

Kalkan, E. Haddadi, H. and Shakal T. (2006). "Seismic input energy of ground motions during the 2004 (M6.0) Parkfield, California earthquake", *Proceedings of the Eight National Earthquake Engineering Conference*, April 18–22, San Francisco.

Kunnath, S. K., Nghiem, Q. and El-Tawil, S. (2004). "Modeling and response prediction in performance-based seismic evaluation: case studies of instrumented steel moment-frame buildings", *Earthquake Spectra*, Vol. 20, No. 3, pp. 883–915.

Leelataviwat, S, Goel, S. C. and Stojadinovic, B. (2002). "Energy-based seismic design of structures using yield mechanism and target drift", J*ournal of Structural Engineering,* ASCE, Vol. 28, No. 8. pp. 1046–1054.

Mahin, S. A. and Lin, J. (1983). *Construction of Inelastic Response Spectrum for Single Degree of Freedom System*. Report No. UCB/EERC-83/17, Earthquake Engineering Research Center, Berkeley, Calif.

Makris, N. and Black, C. (2004). "Evaluation of peak ground velocity as a 'good' intensity measure for near-source ground motions", *Journal of Engineering Mechanics*, ASCE, Vol. 130, No. 9, pp. 1032–1044.

Mavroeidis, G. P., Dong, G. and Papageorgiou, A. S. (2004). Near-fault ground motions, and the response of elastic and inelastic single-degree-freedom (SDOF) systems. *Earthquake Engineering and Structural Dynamics*, Vol. 33, pp. 1023–1049.

McCabe, S. L. and Hall, W. J. (1989). "Assessment of seismic structural damage", *Journal of Structural Engineering,* ASCE, Vol. 115, pp. 2166–2183.

Minami, T. and Osawa, Y. "Elastic-plastic response spectra for different hysteretic rules", *Earthquake Engineering and Structural Dynamics*, Vol. 16. pp. 555–568.

Ordaz, M., Huerta, B. and Reinoso, E. (1999). "Exact computation of input-energy spectra from Fourier amplitude spectra", *Earthquake Engineering and Structural Dynamics*, Vol. 32, No. 4, pp. 597–605.

Otani, S. and Ye, L. (1999). "Maximum seismic displacement of inelastic systems based on energy concept", *Earthquake Engineering and Structural Dynamics*, Vol. 28, pp. 1483–1499.

Park, Y. J., Ang, A. H. S. and Yen, Y. K. (1984). *Seismic Damage Analysis and Damage-limiting Design of RC Buildings*. Civil Engineering Series, UIUC.

Riddell, R. and Garcia, E. J. (2001). "Hysteretic energy spectrum and damage control", *Earthquake Engineering and Structural Dynamics*, Vol. 30, pp. 1791–1816.

Sasani, M. and Bertero, V. V. (2000). "Importance of severe pulse-type ground motions in performance-based engineering: historical and critical review", *Proceedings of the 12th World Conference on Earthquake Engineering*, Paper No. 1302.

Shoji, Y., Tanii, K. and Kamiyama, M. A . (2005). "Study on the duration and amplitude characteristics of earthquake ground motions", *Soil Dynamics and Earthquake Engineering*, Vol. 7-10, pp. 505–512.

Sucuoglu, H., Yucemen, S., Gezer, A. and Erberik, A. Statistical evaluation of the damage potential of earthquake ground motions. *Structural Safety*, Vol. 20, pp. 357–378.

Takahashi, R. (1956). "The SMAC strong motion accelerograph and other latest instruments for measuring earthquakes and building vibrations", *Proceedings of the 1st World Conference on Earthquake Engineering*, Berkeley, CA. Vol. 3**,** pp. 1–11.

Takewaki, I. (2004). "Bound of earthquake input energy", *Journal of. Structural Engineering,* ASCE, Vol. 130, pp. 1289–1297.

Tembulkar, J. M. and Nau, J. M. (1987). "Inelastic modeling and seismic energy dissipation", *Journal of Structual Engineering*, ASCE, Vol. 113, pp. 1373–1377.

Teran-Gilmore, A. (1998). "A parametric approach to performance-based numerical seismic design", *Earthquake Spectra*, Vol. 14, No. 3, pp. 501–520.

Trifunac, M. D. and Brady, A. G. (1975). "On the correlation of seismic intensity scales with the peaks of recorded ground motion", *Bulletin of the Seismological Society of America*, Vol. 65, pp. 139–162.

Uang, C. M. and Bertero, V. V. (1990). "Evaluation of seismic energy in structures", *Earthquake Engineering and Structural Dynamics*, Vol. 19, pp. 77–90.